Preprocedural physiological assessment of coronary disease patterns to predict haemodynamic outcomes post-PCI

Nozomi Kotoku[1], MD; Kai Ninomiya[1], MD; Shinichiro Masuda[1], MD; Neil O'Leary[1], PhD; Scot Garg[2,3], MD, PhD; Mareka Naito[1], MD; Kotaro Miyashita[1], MD; Akihiro Tobe[1], MD; Shigetaka Kageyama[1], MD; Tsung Ying Tsai[1], MD; Pruthvi C. Revaiah[1], MD; Shengxian Tu[4], PhD; Ken Kozuma[5], MD, PhD; Hideyuki Kawashima[5], MD, PhD; Yuki Ishibashi[6], MD, PhD; Gaku Nakazawa[7], MD, PhD; Kuniaki Takahashi[7], MD, PhD; Takayuki Okamura[8], MD, PhD; Yosuke Miyazaki[8], MD, PhD; Hiroki Tateishi[8,9], MD, PhD; Masato Nakamura[10], MD, PhD; Norihiro Kogame[10,11], MD, PhD; Taku Asano[12], MD, PhD; Shimpei Nakatani[13], MD, PhD; Yoshihiro Morino[14], MD, PhD; Masaru Ishida[14], MD, PhD; Yuki Katagiri[15], MD, PhD; Masafumi Ono[12], MD, PhD; Hironori Hara[16], MD; Yohei Sotomi[17], MD, PhD; Kengo Tanabe[18], MD, PhD; Yukio Ozaki[19], MD, PhD; Takashi Muramatsu[20], MD, PhD; Jouke Dijkstra[21], PhD; Yoshinobu Onuma[1], MD, PhD; Patrick W. Serruys[1]*, MD, PhD; on behalf of the ASET-JAPAN investigators

The authors' affiliations can be found in the Appendix paragraph.

This paper also includes supplementary data published online at: https://eurointervention.pcronline.com/doi/10.4244/EIJ-D-23-00516

N. Kotoku and K. Ninomiya contributed equally to this manuscript.

KEYWORDS

- drug-eluting stent
- fractional flow reserve
- intravascular ultrasound
- optical coherence tomography
- stable angina

Abstract

Background: Even with intracoronary imaging-guided stent optimisation, suboptimal haemodynamic outcomes post-percutaneous coronary intervention (PCI) can be related to residual lesions in non-stented segments. Preprocedural assessment of pathophysiological coronary artery disease (CAD) patterns could help predict the physiological response to PCI.

Aims: The aim of this study was to assess the relationship between preprocedural pathophysiological haemodynamic patterns and intracoronary imaging findings, as well as their association with physiological outcomes immediately post-PCI.

Methods: Data from 206 patients with chronic coronary syndrome enrolled in the ASET-JAPAN study were analysed. Pathophysiological CAD patterns were characterised using Murray law-based quantitative flow ratio (μQFR)-derived indices acquired from pre-PCI angiograms. The diffuseness of CAD was defined by the pullback pressure gradient (PPG) index. Intracoronary imaging in stented segments after stent optimisation was also analysed.

Results: In the multivariable analysis, diffuse disease − defined by the pre-PCI μQFR-PPG index − was an independent factor for predicting a post-PCI μQFR <0.91 (per 0.1 decrease of PPG index, odds ratio 1.57, 95% confidence interval: 1.07-2.34; p=0.022), whereas the stent expansion index (EI) was not associated with a suboptimal post-PCI μQFR. Among vessels with an EI ≥80% and post-PCI μQFR <0.91, 84.0% of those vessels had a diffuse pattern preprocedure. There was no significant difference in EI between vessels with diffuse disease and those with focal disease. The average plaque burden in the stented segment was significantly larger in vessels with a preprocedural diffuse CAD pattern.

Conclusions: A physiological diffuse pattern preprocedure was an independent factor in predicting unfavourable immediate haemodynamic outcomes post-PCI, even after stent optimisation using intracoronary imaging. Preprocedural assessment of CAD patterns could identify patients who are likely to exhibit superior immediate haemodynamic outcomes following PCI.

Corresponding author: University of Galway, University Road, Galway, H91 TK33, Ireland.
E-mail: patrick.w.j.c.serruys@gmail.com

Abbreviations

CAD	coronary artery disease
dμQFR/ds	instantaneous μQFR ratio gradient per unit length
FFR	fractional flow reserve
IVUS	intravascular ultrasound
MLA	minimal lumen area
MSA	minimal stent area
OCT	optical coherence tomography
PCI	percutaneous coronary intervention
PPG	pullback pressure gradient
QFR	quantitative flow ratio
TSG	trans-stent gradient
μQFR	Murray law-based quantitative flow ratio

Introduction

The goal of coronary stenting is not merely to diminish coronary stenosis but to also improve clinical outcomes. A higher incidence of vessel-oriented adverse events has been reported in vessels with low post-stenting fractional flow reserve (FFR) values[1,2], including angiography-derived FFR[3]. Vessel-level FFR reveals the cumulative haemodynamic impact of atherosclerosis along the whole vessel, whereas post-percutaneous coronary intervention (PCI) FFR reflects residual flow-limiting factors in stented and non-stented segments of the whole target vessel. A suboptimal FFR post-PCI can occur even after optimal stenting due to residual disease in non-stented segments. Therefore, pre-PCI assessment of pathophysiological patterns of coronary atherosclerosis could help predict the physiological response to PCI. Collet et al proposed a pullback pressure gradient (PPG) index derived from a motorised coronary pressure pullback during continuous hyperaemia to quantify the diffuseness of coronary atherosclerosis[4]. Recent studies show that the presence of diffuse patterns of coronary artery disease (CAD), as documented by the PPG index, is associated with both suboptimal post-PCI FFR and adverse clinical outcomes[5,6].

Conversely, lesions in stented segments can be optimised by using intracoronary imaging. Several randomised control trials (RCT) demonstrated that stent optimisation using intracoronary imaging reduces underexpansion, which is associated with an increased risk for target lesion failure such as in-stent restenosis and stent thrombosis, and improves clinical outcomes[7-9]. However, amongst patients with a post-PCI FFR <0.90, intravascular ultrasound (IVUS)-guided PCI failed to improve clinical outcomes[10]. This result does not take into account preprocedural pathophysiological CAD patterns that are associated with a low post-PCI FFR. Studies assessing preprocedural pathophysiological CAD patterns and intracoronary imaging as serial procedures in PCI, as well as showing their association with physiological outcomes post-PCI, are still scarce.

The aim of this study was to assess the relationship between preprocedural pathophysiological CAD patterns and intracoronary imaging, as well as their association with the physiological outcome immediately post-PCI.

Editorial, see page 877

Methods

STUDY POPULATION

This study included 206 consecutive patients with chronic coronary syndrome enrolled in the Acetyl Salicylic Elimination Trial (ASET)-JAPAN Study (Clinical.Trials.gov: NCT05117866). The study design and main results have been previously reported[11,12]. Briefly, the ASET-JAPAN pilot study is a multicentre, single-arm, open-label, proof-of-concept trial, with a stopping rule based on the occurrence of definite stent thrombosis, to demonstrate the feasibility and safety of "aspirin-free" therapy with low-dose prasugrel monotherapy (3.75 mg once daily) following PCI. The study was approved by the certified review board (CRB4180003) at Fujita Health University (Toyoake, Japan) and the local ethics committees at each investigating centre, and all patients provided their written informed consent prior to participation in the study.

PREPROCEDURAL PATHOPHYSIOLOGICAL CHARACTERISATION OF CAD

Pathophysiological CAD patterns were characterised by the preprocedural physiological distribution and local severity of coronary atherosclerosis using Murray law-based quantitative flow ratio (μQFR)-derived indices, acquired from pre-PCI angiograms. μQFR is a novel computational method applied to a single angiographic view that considers side branch diameters in the computation of fractal flow division and has been recently shown to have similar diagnostic accuracy compared with 3-dimensional QFR and a correlation of r=0.90 (p<0.001) and agreement (mean difference 0.00, standard deviation [SD] 0.05; p=0.378; intraclass correlation coefficient for the absolute value=0.91, 95% confidence interval [CI]: 0.89 to 0.92) with wire-based FFR[13-15].

Preprocedural physiological distribution ("diffuseness or focality") of CAD was assessed using the μQFR-PPG index, calculated as follows[4]:

μQFR-PPG index=

$$\frac{\left\{ \frac{Max\ PPG\ 20\ mm}{\Delta \mu QFR\ vessel} + \left(1 - \frac{Length\ with\ functional\ disease\ [mm]}{Total\ vessel\ length\ [mm]} \right) \right\}}{2}$$

Maximal PPG was defined as the maximum μQFR gradient over 20 mm and delta μQFR vessel as 1-vessel μQFR. The length with functional disease was defined as the length, in millimetres, with a μQFR drop ≥0.0015/mm. The total vessel length was defined as the length of the entire interrogated vessel. The physiological distribution of CAD was defined as predominantly diffuse or focal according to a μQFR-PPG index <0.78 or ≥0.78, respectively[5].

The pre-PCI physiological local severity of a lesion was assessed using the μQFR gradient per mm (dμQFR/ds), with a value ≥0.025/mm defining the presence of a "major gradient"[5].

The μQFR-PPG index and dμQFR/ds were used to categorise pathophysiological CAD patterns into 4 groups[5]: predominantly focal (μQFR-PPG index ≥0.78) with (Group 1) or without (Group 2) a major gradient (dμQFR/ds ≥0.025/mm) and predominantly diffuse (μQFR-PPG index <0.78) with (Group 3) or without (Group 4) a major gradient **(Figure 1)**.
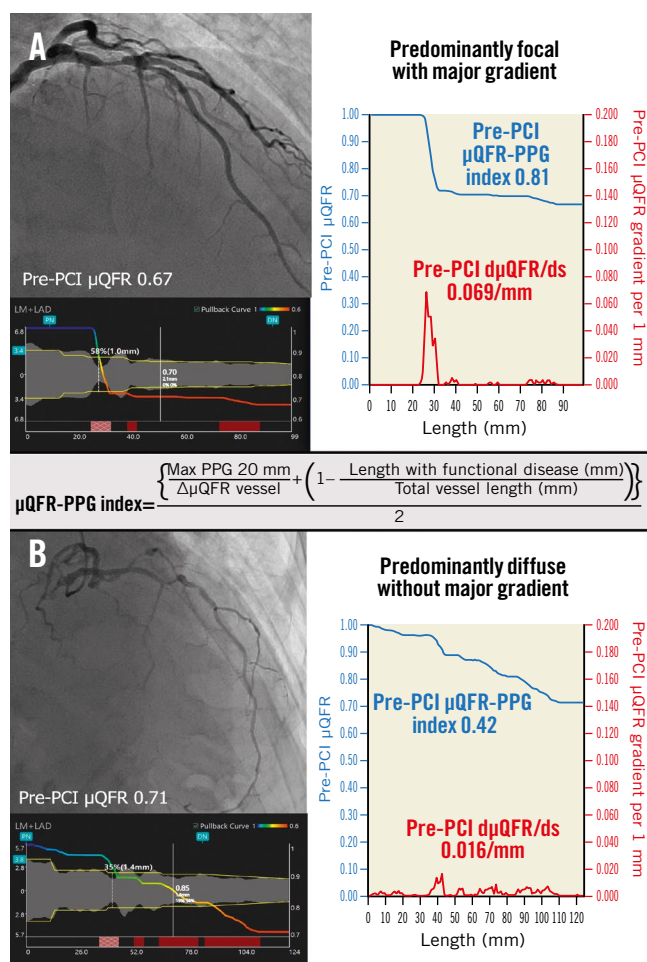
Figure 1. *Pathophysiological CAD patterns assessed by pullback pressure gradient acquired from the pre-PCI angiogram. Red curves in the graphs show pressure drop per 1 mm (dµQFR/ds). Cumulative pressure drop is represented as blue curves. A) The vessel shown has predominantly focal (µQFR-PPG index ≥0.78) disease with a major gradient (dµQFR/ds ≥0.025/mm). B) The vessel shown has predominantly diffuse disease without a major gradient. In this case, the PPG index acquired from the pre-PCI angiogram was 0.42 (<0.78), with the widespread distribution of pressure drop along the target vessel. CAD: coronary artery disease; dµQFR/ ds: instantaneous µQFR ratio gradient per unit length; PCI: percutaneous coronary intervention; PPG: pullback pressure gradient; µQFR: Murray law-based quantitative flow ratio*

ANALYSIS OF µQFR

The independent core laboratory (CORRIB Core Lab, Galway, Ireland) performed the µQFR analysis retrospectively using AngioPlus Core software (version V2, Pulse Medical). Methods to compute µQFR are described in **Supplementary Appendix 1**[3,13]. Contrast flow velocity was automatically converted to hyperaemic flow velocity, and pressure drop was calculated using fluid dynamics equations[13]. A cut-off value of µQFR ≤0.80 was used to indicate a significant flow limitation as a preprocedural physiological assessment[13]. Optimal physiological procedural results were defined as a post-PCI µQFR ≥0.91[3].

The µQFR-based trans-stent gradient (TSG) was defined as ∆µQFR between the proximal and distal stent edges ±5 mm[16]. If a vessel had ≥2 separate stented sites, the µQFR-TSG was calculated as the sum of two or more ∆µQFR[3]. The µQFR gradient in the proximal and distal segments of the stent was also measured.

INTRACORONARY IMAGING ANALYSIS

IVUS and optical coherence tomography (OCT) imaging analyses were performed retrospectively by the aforementioned independent core laboratory offline using dedicated software (Medis v3.1 [Medis Medical Imaging]; QCU-CMS [Leiden University Medical Center]).

A target lesion was defined as a segment including stent and peristent segments of 5 mm proximal and distal to the stent. Whenever paired pullbacks of pre- and postprocedural intravascular imaging were available, the target lesion was matched in the preprocedural images using fiducial landmarks.

On pre-PCI intravascular imaging, the minimal lumen area (MLA) and plaque burden were assessed in the target lesion with a slice thickness of 1.0 mm. The plaque cross-sectional area (CSA) was determined by vessel CSA–lumen CSA. The plaque burden was plaque CSA/vessel CSA multiplied by 100.

On post-PCI intracoronary imaging, the minimal stent area (MSA), stent expansion index, and plaque burden in the target lesion were assessed with a slice thickness of 0.5 mm. The stent expansion index was defined as the MSA divided by the average of the proximal and distal reference lumen areas multiplied by 100 and evaluated with a cut-off value of 80%. In the case of a vessel with more than 1 lesion, data on the lesion with a smaller MSA were used for the statistical analysis. The reference lumen area was defined as an average of 5 mm proximal and distal to the implanted stent[17].

In non-stented segments, the MLA and plaque burden were also analysed with a slice thickness of 1.0 mm in post-PCI intracoronary imaging. The non-stented segment length had to be ≥5 mm in order to be included in the analysis. When the target lesion was in the left anterior descending or circumflex artery, the non-stented proximal segment was analysed up to its ostium **(Supplementary Figure 1)**.

To investigate the difference in the plaque composition between diffuse and focal disease, the automated quantitative echogenicity of plaque components was analysed in the target lesion (preprocedure) and in non-stented segments (post-procedure) observed by IVUS **(Supplementary Appendix 2, Supplementary Figure 2)**[18].

STATISTICAL ANALYSIS

The primary endpoint of the present analysis was haemodynamic outcome post-PCI: optimal and suboptimal haemodynamic outcomes were defined by a post-PCI µQFR ≥0.91 and <0.91, respectively. To predict the unadjusted and adjusted risks of a post-PCI µQFR <0.91, we used binary logistic regression models with preprocedural µQFR, µQFR-PPG index, dµQFR/ds, and stent expansion index as continuous or categorical predictor variables.

To better represent the shape of the association between the suboptimal haemodynamic outcome post-PCI (µQFR <0.91) and

pathophysiological characteristics, preprocedural μQFR, μQFR-PPG index, dμQFR/ds, and stent expansion index, these predictor variables were considered to be continuous variables, and odds ratios (OR) were modelled using a restricted cubic spline curve (3 knots) derived from the unadjusted proportional odds model with the reference of the mean for each variable.

Intracoronary imaging findings were compared between vessels with a diffuse pattern and those with a focal pattern. To estimate 95% confidence intervals for differences, bootstrapping was used with 2000 replications.

Continuous variables are presented as mean and SD or as median and interquartile range (IQR) depending on their distribution and were compared using the Student's t-test or Mann-Whitney U test. Categorical variables are described as percentages.

A 2-sided p-value<0.05 was considered statistically significant. All statistical analyses were performed using R version 4.1.3 (R Foundation for Statistical Computing) and SPSS version 27.0 (IBM).

Results

A total of 206 patients with 217 vessels were enrolled from 12 centres in Japan. Baseline clinical, angiographic, and procedural characteristics are shown in **Supplementary Table 1**. In this study, pre-PCI μQFR was analysed in 207 vessels; 10 vessels with Thrombolysis in Myocardial Infarction (TIMI) flow <3 could not be processed. All 217 post-PCI μQFRs were analysable, resulting in 207 vessels with paired pre- and post-PCI μQFR. In 217 vessels, either post-PCI IVUS or OCT/optical frequency domain imaging (OFDI) was acquired in 147 vessels and 69 vessels and analysable in 143 vessels and 59 vessels, respectively. A total of 193 vessels were analysable both in pre-PCI μQFR-PPG index and post-PCI intracoronary imaging (IVUS: 140 vessels; OCT/OFDI: 53 vessels). Pre-PCI IVUS or OCT/OFDI images were successfully colocalised with the target lesion in post-PCI intracoronary imaging in 101 vessels and 32 vessels, respectively.

PREVALENCE OF PREPROCEDURAL PATHOPHYSIOLOGICAL DISTRIBUTION AND LOCAL SEVERITY

The mean pre-PCI μQFR was 0.67 (SD 0.16) (median 0.71 [IQR 0.58-078]). The mean μQFR-PPG index was 0.68 (SD 0.13) (median 0.68 [IQR 0.60-0.79]). The mean highest dμQFR/ds in each vessel was 0.059/mm (SD 0.045) (median 0.045/mm [IQR 0.029-0.077]).

Pathophysiological CAD patterns in 207 vessels were predominantly focal (μQFR-PPG index ≥0.78) with (Group 1: 26.6%, n=55) or without (Group 2: 1.0%, n=2) a major gradient (dμQFR/ds ≥0.025/mm) and predominantly diffuse (μQFR-PPG index <0.78) with (Group 3: 53.6%, n=111) or without (Group 4: 18.8%, n=39) a major gradient **(Figure 2A)**.

INTRACORONARY IMAGING RESULTS ACCORDING TO THE DIFFUSENESS OF CAD PRE-PCI

The difference in results of intracoronary imaging between vessels with diffuse disease (μQFR-PPG index <0.78) and those with

focal disease (≥0.78) are shown in **Table 1**. In a baseline lesion assessment pre-procedure, the average plaque burden was significantly larger in vessels with diffuse disease than in those with focal disease (53.7% [SD 7.5] vs 50.9% [SD 5.3], mean difference −2.741, 95% CI: −4.817 to −0.800), whereas there was no significant difference in the MLA (2.13 mm^2 [SD 0.92] vs 2.29 mm^2 [SD 1.05], mean difference 0.156, 95% CI: −0.164 to 0.506).

In post-PCI intracoronary imaging, the MSA was significantly smaller in vessels with diffuse disease than in those with focal disease (5.58 mm^2 [SD 2.31] vs 6.67 mm^2 [SD 2.61], mean difference 1.086, 95% CI: 0.437 to 1.774), while the average of the proximal and distal reference lumen areas was also significantly smaller (6.95 mm^2 [SD 3.08] vs 8.32 mm^2 [SD 3.39], mean difference 1.371, 95% CI: 0.537 to 2.231). For the stent expansion index, there was no significant difference between vessels with diffuse disease and those with focal disease (83.3% [SD 18.2] vs 82.0% [SD 15.5], mean difference −1.246%, 95% CI: −5.565 to 3.003). Consistent with the pre-PCI assessment, the average plaque burden in the stented segment was significantly larger in vessels with diffuse disease than in those with focal disease (46.3% [SD 7.6] vs 44.2% [SD 7.0], mean difference −2.199%, 95% CI: −4.114 to −0.293). As expected, the stent length was significantly longer in vessels with diffuse disease than in those with focal disease (28.1 mm [SD 12.3] vs 24.4 mm [SD 8.5], mean difference −3.765, 95% CI: −6.289 to −1.255).

Non-stented segments proximal and distal to the stented segment were analysable (≥5 mm) in 108 vessels and 141 vessels with a mean analysable length of 11.5 mm (SD 15.2) and 9.1 mm (SD 6.4), respectively. The average plaque burden of non-stented segments tended to be larger in vessels with diffuse disease than in those with focal disease (proximal segment 49.4% [SD 10.4] vs 46.3% [SD 8.3], mean difference −3.120, 95% CI: −6.298 to −0.051; distal segment 41.5% [SD 11.8] vs 38.0% [SD 11.4], mean difference −3.433, 95% CI: −6.840 to 0.109) **(Supplementary Table 2)**.

There were no significant differences in plaque components quantified by echogenicity in target lesions and non-stented segments observed by IVUS between vessels with diffuse disease and those with focal disease **(Supplementary Table 3, Supplementary Table 4)**.

ASSOCIATION OF PRE-PCI PATHOPHYSIOLOGICAL CAD PATTERNS AND STENT EXPANSION INDEX WITH A POST-PCI μQFR <0.91

The median post-PCI μQFR was 0.94 (IQR 0.91-0.96, mean 0.93 [SD 0.05]) **(Supplementary Figure 3A)**. In 207 vessels with paired pre- and post-PCI μQFR, the μQFR significantly improved from 0.71 (IQR 0.58-0.78) to 0.94 (IQR 0.91-0.96) (p<0.001) **(Supplementary Figure 3B, Supplementary Figure 3C)**.

The median μQFR-TSG was 0.00 (IQR 0.00-0.01) **(Supplementary Figure 4A)**. The value of the μQFR-TSG was 0.00-0.01 in 85.4% (41/48) of vessels with a post-PCI μQFR <0.91, while the rest of the vessels (7/48) had a μQFR-TSG of 0.02-0.04 **(Supplementary Figure 4B)**. Among 48 vessels with a post-PCI

A

Pathophysiological CAD patterns derived from pre-PCI angiography

B

Relationship between diffuseness of CAD and stent expansion index
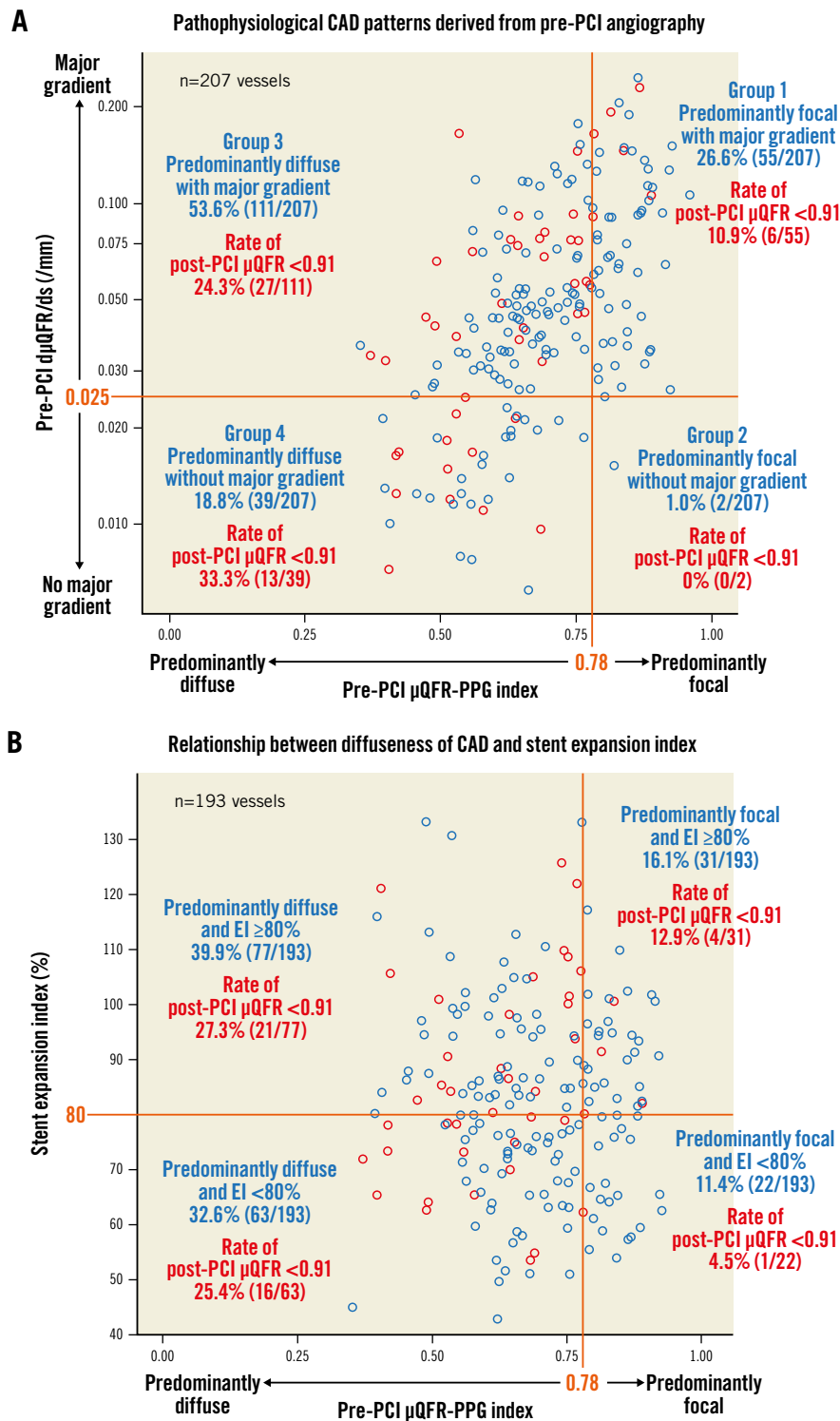
Figure 2. *Pathophysiological CAD patterns and the relationship between diffuseness of CAD and stent expansion index. The x-axis in both figures shows the pre-PCI PPG index derived from pre-PCI angiography. Red and blue open circles show vessels with post-PCI μQFR <0.91 and ≥0.91, respectively. A) The figure shows pathophysiological CAD patterns derived from pre-PCI angiography. On the y-axis, values of dμQFR/ds were plotted in a log scale with absolute values. B) The figure shows the relationship between the diffuseness of CAD and the stent expansion index. CAD: coronary artery disease; dμQFR/ds: instantaneous μQFR ratio gradient per unit length; EI: expansion index; PCI: percutaneous coronary intervention; PPG: pullback pressure gradient; μQFR: Murray law-based quantitative flow ratio*

μQFR <0.91, the median μQFR gradient in the proximal and distal segment of the stent was 0.05 (IQR 0.02-0.10) and 0.08 (IQR 0.04-0.11), respectively. Among those vessels, a μQFR gradient ≥0.04[19] was observed in the proximal segment of the stent in 62.5% (30/48) and in the distal segment of the stent in 79.2% (38/48) of the vessels. Of note, 41.7% (20/48) of those vessels had a μQFR gradient

Table 1. Differences in target lesions observed by intracoronary imaging.

	Vessels with diffuse disease	Vessels with focal disease	Mean difference (95% CI)[a]
Pre-PCI intracoronary imaging	**(n=101)**	**(n=32)**	
MLA, mm² (SD)	2.13 (0.92)	2.29 (1.05)	0.156 (–0.164 to 0.506)
IVUS-derived (n=92)	2.32 (0.91)	2.58 (1.04)	0.250 (–0.114 to 0.645)
OCT-derived (n=41)	1.71 (0.82)	1.42 (0.69)	–0.180 (–0.589 to 0.258)
Average plaque burden, % (SD)	53.7 (7.5)	50.9 (5.3)	–2.741 (–4.817 to –0.800)[†]
Post-PCI intracoronary imaging	**(n=140)**	**(n=53)**	
Reference lumen area, mm² (SD)	6.95 (3.08)	8.32 (3.39)	1.371 (0.537 to 2.231)[†]
IVUS-derived (n=134)	7.01 (3.17)	8.35 (3.68)	1.355 (0.282 to 2.412)[†]
OCT-derived (n=59)	6.83 (2.90)	8.24 (2.55)	1.369 (0.083 to 2.647)[†]
MSA, mm² (SD)	5.58 (2.31)	6.67 (2.61)	1.086 (0.437 to 1.774)[†]
IVUS-derived (n=134)	5.43 (2.24)	6.39 (2.69)	0.970 (0.232 to 1.809)[†]
OCT-derived (n=59)	5.88 (2.46)	7.45 (2.29)	1.560 (0.443 to 2.700)[†]
MSA ≥5.5 mm² for IVUS, MSA ≥4.5 mm² for OCT, % (n)	45.7 (64)	67.9 (36)	22.715 (9.205 to 35.216)[†]
Stent expansion index, % (SD)	83.3 (18.2)	82.0 (15.5)	–1.246 (–5.565 to 3.003)
Stent expansion index ≥80%, % (n)	55.0 (77)	58.5 (31)	3.495 (–9.515 to 17.016)
Average plaque burden, % (SD)	46.3 (7.6)	44.2 (7.0)	–2.199 (–4.114 to –0.293)[†]
Stent length, mm (SD)	28.1 (12.3)	24.4 (8.5)	–3.765 (–6.289 to –1.255)[†]

Diffuse disease and focal disease were defined according to a μQFR-PPG index <0.78 or ≥0.78, respectively. Continuous variables are presented as mean and standard deviation (SD). [a] Confidence intervals (CI) for differences in the mean value were estimated by bootstrapping using 2,000 replications. The cross (†) after 95% CI shows a significant difference. IVUS: intravascular ultrasound; MLA: minimal lumen area; MSA: minimal stent area; OCT: optical coherence tomography; PCI: percutaneous coronary intervention; PPG: pullback pressure gradient; μQFR: Murray law-based quantitative flow ratio

≥0.04 both in the proximal and distal segments of the stent. Among vessels with a post-PCI μQFR <0.91, only 6.3% (3/48) of vessels had a residual major gradient (μQFR/ds ≥0.025/mm).

Vessels with a post-PCI μQFR <0.91 had a significantly smaller MLA in both proximal and distal segments than those with a post-PCI μQFR ≥0.91 (proximal 4.89 mm² [SD 3.10] vs 6.39 mm² [SD 3.36]; p=0.049; distal 3.30 mm² [SD 2.03] vs 4.43 mm² [SD 2.71]; p=0.033), whereas there was no difference in MSA (5.37 mm² [SD 2.02] vs 6.02 mm² [SD 2.53]; p=0.124) **(Supplementary Table 5)**.

There was no significant association between μQFR-TSG and the stent expansion index (TSG=0.0089-0.0004 × stent expansion index [10% increase]; p=0.291). As shown in **Figure 2B**, among vessels with a stent expansion index ≥80%, 23.1% (25/108) of vessels still had a post-PCI μQFR <0.91. Notably, 84.0% (21/25) of those vessels, with a post-PCI μQFR <0.91 despite optimal stent expansion, had predominantly diffuse disease as a preprocedural pathophysiological CAD pattern.

Risks of preprocedural pathophysiological characteristics and stent expansion index for a post-PCI μQFR <0.91 are shown in **Table 2**. Low pre-PCI μQFR values were significantly associated with an increased risk of a post-PCI μQFR <0.91 (per 0.1 decrease of pre-PCI μQFR, OR 1.31, 95% CI: 1.07 to 1.61; p=0.006) **(Figure 3A)**. Similarly, a low PPG index (diffuse disease) showed a significantly higher risk of post-PCI μQFR <0.91 (per 0.1 decrease of the PPG index, OR 1.50, 95% CI: 1.16 to 1.96; p=0.002) **(Figure 3B)**. The highest dμQFR/ds in each vessel

had no significant impact on the risk of a post-PCI μQFR<0.91 (per 0.01 increase of dμQFR/ds, OR 1.02, 95% CI: 0.95 to 1.09; p=0.531) **(Figure 3C)**. The stent expansion index had no significant impact on the risk of a post-PCI μQFR <0.91 (per 10% decrease of the stent expansion index, OR 0.87, 95% CI: 0.71 to 1.06; p=0.163) **(Figure 3D)**.

In the multivariable analysis, a low PPG index was an independent factor for predicting a post-PCI μQFR <0.91 (per 0.1 decrease of the PPG index, OR 1.57, 95% CI: 1.07 to 2.34; p=0.022) **(Table 2)**.

Discussion

The main findings of this study are as follows:

1. In the multivariable analysis, diffuse disease − defined by pre-PCI μQFR-PPG index − was an independent factor for predicting a post-PCI μQFR <0.91 (per 0.1 decrease of the PPG index, OR 1.57, 95% CI: 1.07 to 2.34; p=0.022) whereas the stent expansion index was not associated with a suboptimal post-PCI μQFR.

2. Among vessels with a stent expansion index ≥80%, 23.1% (25/108) of vessels still had a post-PCI μQFR <0.91. Notably, 84.0% (21/25) of those vessels, with a post-PCI μQFR <0.91, despite optimal stent expansion, had predominantly diffuse disease as a preprocedural pathophysiological CAD pattern.

3. There was no significant difference in the stent expansion index between vessels with diffuse disease and those with focal disease. The average plaque burden in the stented segment was significantly larger in vessels with a preprocedural diffuse CAD pattern.

Table 2. Risk for a post-PCI μQFR <0.91.

	Risk for a post-PCI μQFR <0.91			
	Univariable analysis		Multivariable analysis	
Numerical	**OR (95% CI)**	***p*-value**	**OR (95% CI)**	***p*-value**
Pre-PCI μQFR, per 0.1 decrease	1.31 (1.07-1.61)	0.006[†]	1.53 (1.00-2.41)	0.054
Pre-PCI μQFR-PPG index, per 0.1 decrease	1.50 (1.16-1.96)	0.002[†]	1.57 (1.07-2.34)	0.022[†]
Pre-PCI dμQFR/ds, per 0.01/mm increase	1.02 (0.95-1.09)	0.531	0.98 (0.81-1.17)	0.836
Stent expansion index, per 10% decrease	0.87 (0.71-1.06)	0.163	1.14 (0.93-1.40)	0.224
Categorical	**OR (95% CI)**	***p*-value**	**OR (95% CI)**	***p*-value**
Pre-PCI μQFR ≤0.80	2.94 (0.81-18.9)	0.157	–	–
Pre-PCI μQFR-PPG index <0.78	3.09 (1.31-8.53)	0.016[†]	–	–
Pre-PCI dμQFR/ds ≥0.025/mm	0.53 (0.25-1.17)	0.106	–	–
Stent expansion index <80%	0.83 (0.41-1.65)	0.599	–	–

Adjusted covariates included preprocedural μQFR, μQFR-PPG index, dμQFR/ds, and stent expansion index. [†] shows a significant difference.
CI: confidence interval; dμQFR/ds: instantaneous μQFR ratio gradient per unit length; OR: odds ratio; PCI: percutaneous coronary intervention; PPG: pullback pressure gradient; μQFR: Murray law-based quantitative flow ratio

IMPACT OF PREPROCEDURAL PATHOPHYSIOLOGICAL PATTERNS ON IMMEDIATE HAEMODYNAMIC OUTCOMES POST-PCI

Multiple large observational studies and *post hoc* analyses of RCTs have established that post-PCI FFR and angiography-derived FFR were independent predictors of long-term clinical outcomes[1-3,20]. The determinant of achieving optimal haemodynamic PCI results should be multifactorial, and one of the key determinants could be prepathophysiological patterns (focal vs diffuse pattern). Collet et al reported patients with focal disease (wire-based FFR PPG index ≥0.66) treated with PCI had more favourable patient-oriented outcomes (angina frequency, physical limitations, and quality of life) than patients with diffuse disease (<0.66)[21]. More than half of the patients with diffuse disease remained symptomatic after PCI[21].

Recently, Shin et al showed that prepathophysiological patterns could be characterised by QFR virtual pullback without pressure-wire pullback[5]. They also reported that the rate of target vessel failure after PCI was significantly higher in patients with diffuse disease (QFR-based PPG index <0.78) compared with focal disease (≥0.78)[5]. In the present study, diffuse pattern − defined by pre-PCI μQFR-PPG index − was an independent factor for predicting suboptimal haemodynamic PCI results (post-PCI μQFR <0.91), whereas local severity (dμQFR/ds) and stent expansion index were not associated with a suboptimal post-PCI μQFR. Based on a cut-off value of the PPG index of 0.78, vessels with diffuse disease had a 3.09-fold risk of suboptimal haemodynamic PCI results (95% CI: 1.31 to 8.53).

The optimal cut-off value of the PPG index to predict outcomes of PCI remains to be established; however, the findings from this study suggest that, as a continuous metric, a low μQFR-PPG index was an independent factor for predicting suboptimal physiological results immediately after PCI.

RELATIONSHIP BETWEEN MORPHOLOGICAL FINDINGS OBSERVED BY INTRACORONARY IMAGING AND DIFFUSENESS OF CAD

The vessels with a preprocedural diffuse pattern had a smaller MSA than those with a focal pattern. This result was consistent with the previous report by Mizukami et al, although the mechanism has not yet been discussed[22]. Our findings showed that vessels with diffuse disease also had smaller reference lumen areas than those with focal disease. As a result, there was no difference in the stent expansion index between vessels with diffuse versus focal disease. The average plaque burden in a stented segment was significantly larger in vessels with diffuse disease than in those with focal disease, reflecting the widespread plaque along the lesion segment **(Central illustration)**. Considering this result, it is possible that the sites of reference vessel areas also had plaque, with no actual healthy segments around the target lesion, resulting in small reference lumen areas. Sakai et al reported differences in plaque components on OCT images between vessels with diffuse disease and those with focal disease[23]. However, our results did not confirm their finding. There was no significant difference in plaque components quantified by echogenicity in target lesions and non-stented segments on IVUS images between vessels with diffuse disease and those with focal disease.

ROLE OF INTRACORONARY IMAGING

Several RCTs have demonstrated that intracoronary imaging-guided PCI can improve clinical outcomes[7,8]. Therefore, the current European Society of Cardiology (ESC) guideline recommends the use of IVUS/OCT in selected patients to optimise stent implantation (Class IIa)[24]. However, it remains unclear whether stent optimisation using intracoronary imaging can improve haemodynamic outcomes post-PCI and clinical outcomes. In the FFR SEARCH registry, amongst 100 vessels with a post-PCI FFR
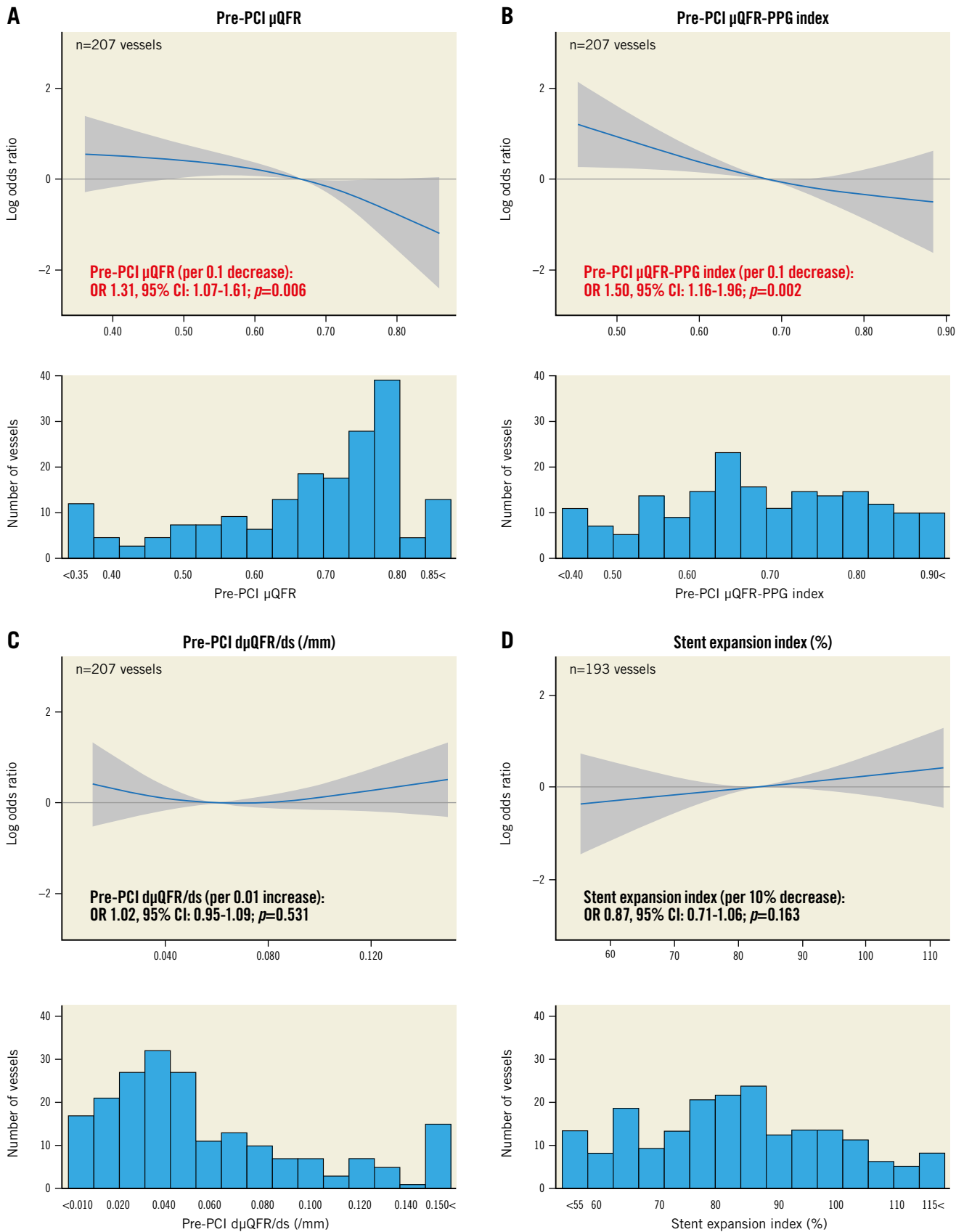
Figure 3. *Risk (odds ratio) for post-PCI µQFR <0.91 with histograms. Spline curves show the risk according to preprocedural µQFR (A), µQFR-PPG index (B), dµQFR/ds (C), and stent expansion index (D). CI: confidence interval; dµQFR/ds: instantaneous µQFR ratio gradient per unit length; OR: odds ratio; PCI: percutaneous coronary intervention; PPG: pullback pressure gradient; µQFR: Murray law-based quantitative flow ratio*

EuroIntervention

CENTRAL **ILLUSTRATION** Importance of assessment of pre-PCI pathophysiological CAD pattern in addition to stent optimisation by intracoronary imaging.
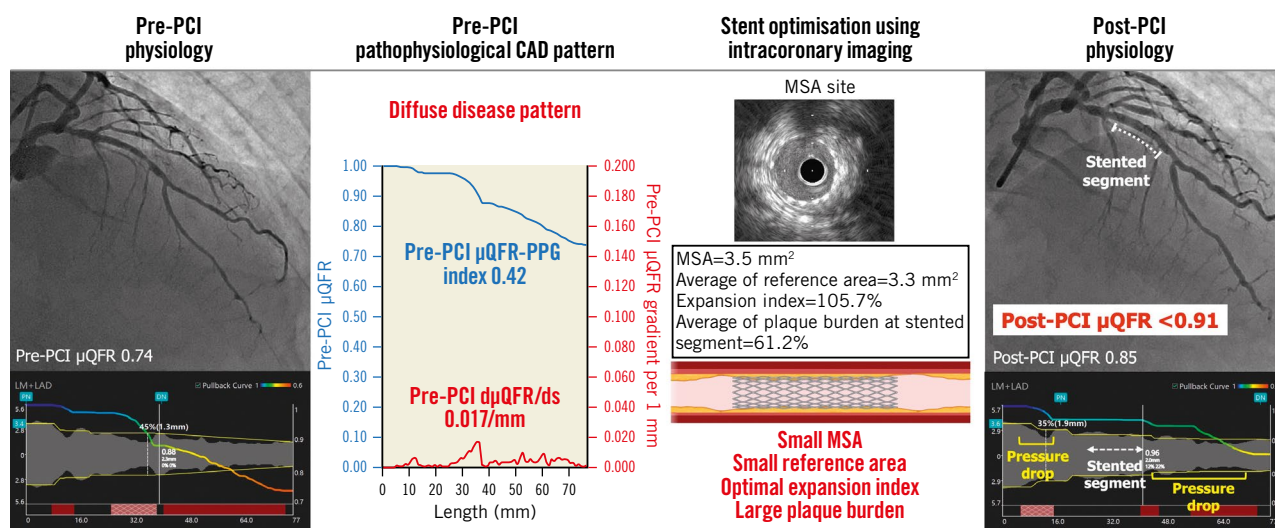
The target vessel with diffuse disease pattern in pre-PCI pathophysiological assessment achieved an expansion index ≥80% by stent optimisation using IVUS. However, the post-PCI μQFR was still <0.91 due to a residual pressure drop in non-stented segments, while the μQFR-trans-stent gradient was 0.00. This case also had characteristics of diffuse disease in intracoronary imaging, such as a small MSA, small reference area, and large plaque burden in the stented segment. CAD: coronary artery disease; dμQFR/ds: instantaneous μQFR ratio gradient per unit length; MSA: minimal stent area; PCI: percutaneous coronary intervention; PPG: pullback pressure gradient; μQFR: Murray law-based quantitative flow ratio

≤0.85, stent underexpansion was found in 74%, and the incidence of stent underexpansion was not different between high and low post-PCI FFR[17]. Stent underexpansion does not necessarily mean the presence of physiologically significant stenosis.

In FFR REACT (FFR-Guided PCI Optimization Directed by High-Definition IVUS Versus Standard of Care), patients with a post-PCI FFR <0.90 at the time of angiographically successful PCI were randomised to IVUS-guided optimisation or the standard of care[10]. The investigators found that stent optimisation guided by IVUS did not improve clinical outcomes compared with the standard of care[10]. This study did not involve an assessment of the preprocedural pathophysiological pattern that is a key predictor of a low post-PCI FFR. As evidenced by the low final post-PCI FFR (0.84) with only a minimal FFR increase (0.03) even after stent optimisation, the majority of the enrolled patients who underwent stent optimisation could have had a diffuse CAD pattern.

In the present study, the stent expansion index was not associated with optimal haemodynamic PCI results. Importantly, among vessels with a stent expansion index ≥80% and a post-PCI μQFR <0.91, 84.0% had predominantly diffuse disease prior to the procedure. The value of the μQFR-TSG was 0.00-0.01 in 85.4% of vessels with a post-PCI μQFR <0.91. The remainder of those vessels also showed a low TSG value of only 0.02-0.04. This result suggests that the majority of the residual pressure drop is out of the stented segment. In addition, 41.7% of vessels with a post-PCI

μQFR <0.91 had a μQFR gradient ≥0.04[19] both in the proximal and distal segments of the stent. This may explain the lack of benefit of stent optimisation by intracoronary imaging. Our findings suggest that haemodynamic outcomes post-PCI are more dependent on the diffuseness of the disease than on stent optimisation by intracoronary imaging **(Central illustration)**.

Consistent with stented segments, the average plaque burden observed by intracoronary imaging in non-stented segments tended to be larger in vessels with diffuse disease than in those with focal disease. However, analysable non-stented segments from clinically obtained intracoronary imaging were limited in length. This reflects the fact that, post-procedure, operators used intracoronary imaging focusing on the stented segments for optimisation, not for detecting residual lesions outside stented segments.

Of note, our results should not question the clinical utility of intracoronary imaging but instead promote the intrinsic clinical value of intracoronary imaging. Since assessment solely based on either intracoronary imaging or physiological assessment, including angiography-derived FFR, cannot detect all the information needed to achieve optimal outcomes after PCI, these techniques could complement each other[25]. Stent-associated complications, such as malapposition and edge dissection, which can only be captured by intracoronary imaging, are associated with long-term clinical outcomes rather than immediate haemodynamic outcomes post-PCI. Furthermore, the computation of the

in-stent angiography-derived FFR gradient can be challenging; wire-based physiological assessment is more sensitive to pressure losses caused by haemodynamic friction, while angiography-derived physiological assessment is particularly sensitive to pressure losses caused by haemodynamic turbulence[26]. Erriquez et al[16] reported the impact of the trans-stent QFR gradient on outcomes after PCI, with a median value of QFR-TSG 0.00 (IQR 0.00-0.01) for all vessels, which is exactly the same as in our study and much lower than TSG based on wire-based FFR assessment (median TSG=0.04)[27].

A comprehensive assessment integrating physiological patterns and intracoronary imaging can better help predict patient risk for major adverse cardiac events and guide more appropriate treatment strategies.

WHAT SHOULD BE THE TREATMENT STRATEGY FOR VESSELS WITH PHYSIOLOGICAL DIFFUSE DISEASE?

The present study demonstrated that diffuse disease, defined by the pre-PCI μQFR-PPG index, was an independent factor for predicting suboptimal haemodynamic outcomes post-PCI. Furthermore, stent optimisation by intracoronary imaging in diffuse disease did not offer an additional benefit.

The AQVA (Angio-based Quantitative Flow Ratio Virtual PCI Versus Conventional Angio-guided PCI in the Achievement of an Optimal Post-PCI QFR) trial suggested that the attention shifted from optimisation based on post-PCI physiological assessment to a better procedural plan based on pre-PCI physiology pullback[28]. It has been also reported that in bypass surgery, physiologically diffuse disease, defined by pressure-wire pullback data, in the recipient coronary artery was associated with an increased risk of graft failure compared to focal disease[29].

Routine assessment of the preprocedural vessel physiology might aid in identifying patients at risk of poor outcomes from PCI and may possibly identify candidates more suitable for pharmacological treatment aimed at regression of diffuse atherosclerosis. The best strategies to treat this physiologically diffuse disease − including novel pharmacological therapy with "powerful antiatherogenic agents" such as micro-RNA, PCSK-9 inhibitors, lipoprotein(a), high-sensitivity C-reactive proteins, and IL-6 − remain to be established[30].

Limitations

The present study must be interpreted with caution due to some limitations. The results of this proof-of-concept study are only hypothesis-generating. Our sample size is limited to 206 Japanese patients, with possible ethnic issues related to anatomy and physiology. Although a diffuse pattern was associated with the immediate haemodynamic outcome post-PCI in the present study, the impact on clinical outcomes was not evaluated. Further clinical studies incorporating both preprocedural pathophysiological CAD patterns and intracoronary imaging assessments are warranted to validate our conclusions and to determine the best strategies for vessels with physiological diffuse disease.

Conclusions

The preprocedural physiological diffuse CAD pattern, characterised by the virtual pullback of FFR derived from angiography, was an independent factor in predicting an unfavourable immediate haemodynamic outcome post-PCI, even after stent optimisation using intracoronary imaging. Preprocedural assessment of the disease pattern of CAD can help to predict the physiological response to PCI and help to identify patients who will benefit from PCI.

Impact on daily practice

A physiological diffuse pattern of CAD preprocedure was an independent factor in predicting unfavourable immediate haemodynamic outcomes post-PCI, even after stent optimisation using intracoronary imaging. Evaluation of the disease pattern of CAD prior to the procedure assists in predicting the physiological response to PCI and identifying individuals who will benefit from PCI. A comprehensive assessment integrating physiological patterns and intracoronary imaging can better help predict patient risk and guide more appropriate treatment strategies. The best strategies to treat a vessel with physiological diffuse disease, including long-term pharmacological treatments aimed at regressing diffuse atherosclerosis, warrant further exploration.

Appendix. Authors' affiliations

1. Department of Cardiology, University of Galway, Galway, Ireland; 2. Department of Cardiology, Royal Blackburn Hospital, Blackburn, United Kingdom; 3. School of Medicine, University of Central Lancashire, Preston, United Kingdom; 4. School of Biomedical Engineering, Shanghai Jiao Tong University, Shanghai, China; 5. Department of Cardiology, Teikyo University Hospital, Tokyo, Japan; 6. Division of Cardiology, Department of Internal Medicine, St. Marianna University School of Medicine, Kanagawa, Japan; 7. Department of Cardiology, Kindai University Faculty of Medicine, Osaka, Japan; 8. Division of Cardiology, Department of Medicine and Clinical Science, Yamaguchi University, Graduate School of Medicine, Yamaguchi, Japan; 9. Department of Cardiology, Shibata Hospital, Yamaguchi, Japan; 10. Division of Cardiovascular Medicine, Toho University Ohashi Medical Center, Tokyo, Japan; 11. Department of Cardiology, Tokyo Rosai Hospital, Tokyo, Japan; 12. Department of Cardiology, St. Luke's International Hospital, Tokyo, Japan; 13. Department of Cardiology, JCHO, Hoshigaoka Medical Center, Osaka, Japan; 14. Department of Cardiology, Iwate Medical University Hospital, Iwate, Japan; 15. Department of Cardiology, Sapporo Higashi Tokushukai Hospital, Hokkaido, Japan; 16. Department of Cardiology, The University of Tokyo Hospital, Tokyo, Japan; 17. Department of Cardiovascular Medicine, Osaka University, Graduate School of Medicine, Osaka, Japan; 18. Division of Cardiology, Mitsui Memorial Hospital, Tokyo, Japan; 19. Department of Cardiology, Fujita Health University Okazaki Medical Center, Aichi, Japan; 20. Department

of Cardiology, Fujita Health University Hospital, Toyoake, Japan; 21. Division of Image Processing, Department of Radiology, Leiden University Medical Center, Leiden, the Netherlands

References

1. Diletti R, Masdjedi K, Daemen J, van Zandvoort LJC, Neleman T, Wilschut J, Den Dekker WK, van Bommel RJ, Lemmert M, Kardys I, Cummins P, de Jaegere P, Zijlstra F, Van Mieghem NM. Impact of Poststenting Fractional Flow Reserve on Long-Term Clinical Outcomes: The FFR-SEARCH Study. *Circ Cardiovasc Interv.* 2021;14:e009681.

2. Piroth Z, Toth GG, Tonino PAL, Barbato E, Aghlmandi S, Curzen N, Rioufol G, Pijls NHJ, Fearon WF, Jüni P, De Bruyne B. Prognostic Value of Fractional Flow Reserve Measured Immediately After Drug-Eluting Stent Implantation. *Circ Cardiovasc Interv.* 2017;10:e005233.

3. Kogame N, Takahashi K, Tomaniak M, Chichareon P, Modolo R, Chang CC, Komiyama H, Katagiri Y, Asano T, Stables R, Fath-Ordoubadi F, Walsh S, Sabaté M, Davies JE, Piek JJ, van Geuns RJ, Reiber JHC, Banning AP, Escaned J, Farooq V, Serruys PW, Onuma Y. Clinical Implication of Quantitative Flow Ratio After Percutaneous Coronary Intervention for 3-Vessel Disease. *JACC Cardiovasc Interv.* 2019;12:2064-75.

4. Collet C, Sonck J, Vandeloo B, Mizukami T, Roosens B, Lochy S, Argacha JF, Schoors D, Colaiori I, Di Gioia G, Kodeboina M, Suzuki H, Van 't Veer M, Bartunek J, Barbato E, Cosyns B, De Bruyne B. Measurement of Hyperemic Pullback Pressure Gradients to Characterize Patterns of Coronary Atherosclerosis. *J Am Coll Cardiol.* 2019;74:1772-84.

5. Shin D, Dai N, Lee SH, Choi KH, Lefieux A, Molony D, Hwang D, Kim HK, Jeon KH, Lee HJ, Jang HJ, Ha SJ, Park TK, Yang JH, Song YB, Hahn JY, Choi SH, Doh JH, Shin ES, Nam CW, Koo BK, Gwon HC, Ge J, Lee JM. Physiological Distribution and Local Severity of Coronary Artery Disease and Outcomes After Percutaneous Coronary Intervention. *JACC Cardiovasc Interv.* 2021;14:1771-85.

6. Dai N, Zhang R, Hu N, Guan C, Zou T, Qiao Z, Zhang M, Duan S, Xie L, Dou K, Zhang Y, Xu B, Ge J. Integrated coronary disease burden and patterns to discriminate vessels benefiting from percutaneous coronary intervention. *Catheter Cardiovasc Interv.* 2022;99:E12-21.

7. Zhang J, Gao X, Kan J, Ge Z, Han L, Lu S, Tian N, Lin S, Lu Q, Wu X, Li Q, Liu Z, Chen Y, Qian X, Wang J, Chai D, Chen C, Li X, Gogas BD, Pan T, Shan S, Ye F, Chen SL. Intravascular Ultrasound Versus Angiography-Guided Drug-Eluting Stent Implantation: The ULTIMATE Trial. *J Am Coll Cardiol.* 2018;72:3126-37.

8. Hong SJ, Kim BK, Shin DH, Nam CM, Kim JS, Ko YG, Choi D, Kang TS, Kang WC, Her AY, Kim YH, Hur SH, Hong BK, Kwon H, Jang Y, Hong MK; IVUS-XPL Investigators. Effect of Intravascular Ultrasound-Guided vs Angiography-Guided Everolimus-Eluting Stent Implantation: The IVUS-XPL Randomized Clinical Trial. *JAMA.* 2015;314:2155-63.

9. Adriaenssens T, Joner M, Godschalk TC, Malik N, Alfonso F, Xhepa E, De Cock D, Komukai K, Tada T, Cuesta J, Sirbu V, Feldman LJ, Neumann FJ, Goodall AH, Heestermans T, Buysschaert I, Hlinomaz O, Belmans A, Desmet W, Ten Berg JM, Gershlick AH, Massberg S, Kastrati A, Guagliumi G, Byrne RA; Prevention of Late Stent Thrombosis by an Interdisciplinary Global European Effort (PRESTIGE) Investigators. Optical Coherence Tomography Findings in Patients With Coronary Stent Thrombosis: A Report of the PRESTIGE Consortium (Prevention of Late Stent Thrombosis by an Interdisciplinary Global European Effort). *Circulation.* 2017;136:1007-21.

10. Neleman T, van Zandvoort LJC, Tovar Forero MN, Masdjedi K, Ligthart JMR, Witberg KT, Groenland FTW, Cummins P, Lenzen MJ, Boersma E, Nuis RJ, den Dekker WK, Diletti R, Wilschut J, Zijlstra F, Van Mieghem NM, Daemen J. FFR-Guided PCI Optimization Directed by High-Definition IVUS Versus Standard of Care: The FFR REACT Trial. *JACC Cardiovasc Interv.* 2022;15:1595-607.

11. Masuda S, Muramatsu T, Ishibashi Y, Kozuma K, Tanabe K, Nakatani S, Kogame N, Nakamura M, Asano T, Okamura T, Miyazaki Y, Tateishi H, Ozaki Y, Nakazawa G, Morino Y, Katagiri Y, Garg S, Hara H, Ono M, Kawashima H, Lemos PA, Serruys PW, Onuma Y. Reduced-dose prasugrel monotherapy without aspirin after PCI with the SYNERGY stent in East Asian patients presenting with chronic coronary syndromes or non-ST-elevation acute coronary syndromes: rationale and design of the ASET Japan pilot study. *AsiaIntervention.* 2023;9:39-48.

12. Muramatsu T, Masuda S, Kotoku N, Kozuma K, Kawashima H, Ishibashi Y, Nakazawa G, Takahashi K, Okamura T, Miyazaki Y, Tateishi H, Nakamura M, Kogame N, Asano T, Nakatani S, Morino Y, Katagiri Y, Ninomiya K, Kageyama S, Takahashi H, Garg S, Tu S, Tanabe K, Ozaki Y, Serruys PW, Onuma Y. Prasugrel Monotherapy After Percutaneous Coronary Intervention With Biodegradable-Polymer Platinum-Chromium Everolimus Eluting Stent for Japanese Patients With Chronic Coronary Syndrome (ASET-JAPAN). *Circ J.* 2023;87:857-65.

13. Tu S, Ding D, Chang Y, Li C, Wijns W, Xu B. Diagnostic accuracy of quantitative flow ratio for assessment of coronary stenosis significance from a single angiographic view: A novel method based on bifurcation fractal law. *Catheter Cardiovasc Interv.* 2021;97:1040-7.

14. Ding D, Tu S, Chang Y, Li C, Xu B and Wijns W. Quantitative Flow Ratio Based on Murray Fractal Law: Accuracy of Single Versus Two Angiographic Views. *JSCAI.* 2022;1:100399.

15. Wang HY, Zhang R, Dou K, Huang Y, Xie L, Qiao Z, Zou T, Guan C, Song L, Yang W, Wu Y, Tu S, Wijns W, Xu B. Left main bifurcation stenting: impact of residual ischaemia on cardiovascular mortality. *Eur Heart J.* 2023;44:4324-36.

16. Erriquez A, Uretsky BF, Brugaletta S, Spitaleri G, Cerrato E, Quadri G, Manfrini M, Pompei G, Scancarello D, Trichilo M, Marchini F, Caglioni S, Campana R, Marrone A, Penzo C, Tumscitz C, Tebaldi M, Verardi FM, Scala A, Campo G, Biscaglia S. Impact of trans-stent gradient on outcome after PCI: results from a HAWKEYE substudy. *Int J Cardiovasc Imaging.* 2022;38:2819-27.

17. van Zandvoort LJC, Masdjedi K, Witberg K, Ligthart J, Tovar Forero MN, Diletti R, Lemmert ME, Wilschut J, de Jaegere PPT, Boersma E, Zijlstra F, Van Mieghem NM, Daemen J. Explanation of Postprocedural Fractional Flow Reserve Below 0.85. *Circ Cardiovasc Interv.* 2019;12:e007030.

18. Bruining N, Verheye S, Knaapen M, Somers P, Roelandt JR, Regar E, Heller I, de Winter S, Ligthart J, Van Langenhove G, de Feijter PJ, Serruys PW, Hamers R. Three-dimensional and quantitative analysis of atherosclerotic plaque composition by automated differential echogenicity. *Catheter Cardiovasc Interv.* 2007;70:968-78.

19. De Bruyne B, Hersbach F, Pijls NH, Bartunek J, Bech JW, Heyndrickx GR, Gould KL, Wijns W. Abnormal epicardial coronary resistance in patients with diffuse atherosclerosis but "Normal" coronary angiography. *Circulation.* 2001;104:2401-6.

20. Biscaglia S, Tebaldi M, Brugaletta S, Cerrato E, Erriquez A, Passarini G, Ielasi A, Spitaleri G, Di Girolamo D, Mezzapelle G, Geraci S, Manfrini M, Pavasini R, Barbato E, Campo G. Prognostic Value of QFR Measured Immediately After

Successful Stent Implantation: The International Multicenter Prospective HAWKEYE Study. *JACC Cardiovasc Interv.* 2019;12:2079-88.

21. Collet C, Collison D, Mizukami T, McCartney P, Sonck J, Ford T, Munhoz D, Berry C, De Bruyne B, Oldroyd K. Differential Improvement in Angina and Health-Related Quality of Life After PCI in Focal and Diffuse Coronary Artery Disease. *JACC Cardiovasc Interv.* 2022;15:2506-18.

22. Mizukami T, Sonck J, Sakai K, Ko B, Maeng M, Otake H, Koo BK, Nagumo S, Nørgaard BL, Leipsic J, Shinke T, Munhoz D, Mileva N, Belmonte M, Ohashi H, Barbato E, Johnson NP, De Bruyne B, Collet C. Procedural Outcomes After Percutaneous Coronary Interventions in Focal and Diffuse Coronary Artery Disease. *J Am Heart Assoc.* 2022;11:e026960.

23. Sakai K, Mizukami T, Leipsic J, Belmonte M, Sonck J, Nørgaard BL, Otake H, Ko B, Koo BK, Maeng M, Jensen JM, Buytaert D, Munhoz D, Andreini D, Ohashi H, Shinke T, Taylor CA, Barbato E, Johnson NP, De Bruyne B, Collet C. Coronary Atherosclerosis Phenotypes in Focal and Diffuse Disease. *JACC Cardiovasc Imaging.* 2023;S1936-878X:00274-7.

24. Neumann FJ, Sousa-Uva M, Ahlsson A, Alfonso F, Banning AP, Benedetto U, Byrne RA, Collet JP, Falk V, Head SJ, Jüni P, Kastrati A, Koller A, Kristensen SD, Niebauer J, Richter DJ, Seferovic PM, Sibbing D, Stefanini GG, Windecker S, Yadav R, Zembala MO. 2018 ESC/EACTS Guidelines on myocardial revascularization. *EuroIntervention.* 2019;14:1435-534.

25. Koo BK, Hwang D. Imaging and Physiological Assessment After Stent Implantation. *Circ Cardiovasc Interv.* 2019;12:e007718.

26. Warisawa T, Cook CM, Howard JP, Ahmad Y, Doi S, Nakayama M, Goto S, Yakuta Y, Karube K, Shun-Shin MJ, Petraco R, Sen S, Nijjer S, Al Lamee R, Ishibashi Y, Matsuda H, Escaned J, di Mario C, Francis DP, Akashi YJ, Davies JE. Physiological Pattern of Disease Assessed by Pressure-Wire Pullback Has an Influence on Fractional Flow Reserve/Instantaneous Wave-Free Ratio Discordance. *Circ Cardiovasc Interv.* 2019;12:e007494.

27. Uretsky BF, Agarwal SK, Vallurupalli S, Al-Hawwas M, Miller K, Biscaglia S, Hakeem A. Trans-Stent FFR Gradient as a Modifiable Integrant in Predicting Long-Term Target Vessel Failure. *JACC Cardiovasc Interv.* 2022;15:2192-202.

28. Biscaglia S, Verardi FM, Tebaldi M, Guiducci V, Caglioni S, Campana R, Scala A, Marrone A, Pompei G, Marchini F, Scancarello D, Pignatelli G, D'Amore SM, Colaiori I, Demola P, Di Serafino L, Tumscitz C, Penzo C, Erriquez A, Manfrini M, Campo G. QFR-Based Virtual PCI or Conventional Angiography to Guide PCI: The AQVA Trial. *JACC Cardiovasc Interv.* 2023;16:783-94.

29. Shiono Y, Kubo T, Honda K, Katayama Y, Aoki H, Satogami K, Kashiyama K, Taruya A, Nishiguchi T, Kuroi A, Orii M, Kameyama T, Yamano T, Yamaguchi T, Matsuo Y, Ino Y, Tanaka A, Hozumi T, Nishimura Y, Okamura Y, Akasaka T. Impact of functional focal versus diffuse coronary artery disease on bypass graft patency. *Int J Cardiol.* 2016;222:16-21.

30. Serruys PW, Kageyama S, Garg S, Onuma Y. In the Beginning There Was Angina Pectoris, at the End There Was Still Angina Pectoris. *JACC Cardiovasc Interv.* 2022;15:2519-22.

Supplementary data

Supplementary Appendix 1. Computation methods of Murray law-based quantitative flow ratio (µQFR).

Supplementary Appendix 2. Echogenicity quantification of plaque component observed by IVUS.

Supplementary Table 1. Baseline clinical, angiographic and procedural characteristics.

Supplementary Table 2. Differences in non-stented segments observed by intracoronary imaging.

Supplementary Table 3. Comparison of automated quantitative echogenicity of plaque components in the target lesion between vessels with diffuse disease and those with focal disease.

Supplementary Table 4. Comparison of automated quantitative echogenicity of plaque components in non-stented segments between vessels with diffuse disease and those with focal disease.

Supplementary Table 5. Comparison of MLA in non-stented segments and MSA between vessels with a post-PCI µQFR <0.91 and those with a post-PCI µQFR ≥0.91.

Supplementary Figure 1. Case example of intracoronary imaging analysis in non-stented segments.

Supplementary Figure 2. Example of automated quantitative echogenicity of plaque component observed by IVUS.

Supplementary Figure 3. Assessment of pre- and post-PCI µQFR.

Supplementary Figure 4. Histogram showing the distribution of post-PCI µQFR-TSG.

Supplementary data

Supplementary Appendix 1. Computation methods of Murray law-based quantitative flow ratio (μQFR).

Vessel μQFR was analysed from the ostium of the main vessels (right coronary artery [RCA] or left main coronary artery) until the distal point, defined as an anatomical landmark (i.e., side branch) in the segment in which its diameter became <2.0 mm. If a vessel had ≥2 daughter branches in the distal segment (e.g., right posterior descending artery or posterolateral branch from RCA, left posterolateral or posterior descending artery in left circumflex artery), the vessel with the greater diameter was analysed as the main vessel. The software automatically delineated the lumen contour of the main analysis vessel and all its side branches with diameters of ≥1.0 mm. The lumen contour was corrected manually if needed.

Supplementary Appendix 2. Echogenicity quantification of plaque component observed by IVUS.

The automated quantitative echogenicity of plaque components in target lesions observed by pre-percutaneous coronary intervention (PCI) intravascular ultrasound (IVUS) and in non-stented segments observed by post-PCI IVUS was performed using dedicated software (QCU-CMS, Leiden University Medical Center).[18] Following echogenicity-based tissue components were defined using the reference grey-level intensity of the adventitia: hypo- and hyper-echogenic tissue, calcification, and upper and lower tissue. The calcifications were identified through a combination of highly echogenic tissue accompanied by radial acoustic shadowing.

Supplementary Table 1. Baseline clinical, angiographic and procedural characteristics.

Patient characteristics (n=206 patients)	
Age, years (SD)	69.0 (9.8)
Male, % (n)	81.6 (168)
BMI, kg/m^2 (SD)	24.6 (3.9)
Hypertension, % (n)	80.1 (165)
Diabetes mellitus, % (n)	35.9 (74)
Insulin-dependent, % (n)	7.3 (15)
Dyslipidemia, % (n)	85.4 (176)
Current smoking, % (n)	17.5 (36)
Previous myocardial infarction, % (n)	13.1 (27)
Previous PCI, % (n)	24.8 (51)
Previous CABG, % (n)	1.9 (4)
Left ventricular ejection fraction, % (SD)	60.5 (10.0)
Renal insufficiency [a], % (n)	34.4 (71)
Anatomical SYNTAX score (SD)	8.0 (4.6)
Vessels treated per patient, % (n)	
1 vessel	94.7 (195)
2 vessels	5.3 (11)
Vessel characteristics (n=217 vessels)	
Target vessel, % (n)	
Left main-LAD	1.8 (4)
LAD territory	63.1 (137)
LCX	15.7 (34)
RCA	19.4 (42)
Intravascular imaging device use for stent optimization, % (n)	
No use for imaging modality (angiography alone)	0.5 (1)
IVUS	67.7 (147)
OCT or OFDI	31.8 (69)
Number of stents used per vessel, % (n)	
1 stent	96.8 (210)
2 stents	3.2 (7)
Lesion characteristics (n=224 lesions [b])	

Pre-PCI QCA	
Reference vessel diameter, mm (SD)	2.78 (0.69)
Minimum lumen diameter, mm (SD)	1.12 (0.50)
Diameter stenosis, % (SD)	59 (14)
Lesion length, mm (SD)	14.4 (8.0)
Post-PCI QCA	
Reference vessel diameter, mm (SD)	2.87 (0.66)
Minimum lumen diameter, mm (SD)	2.46 (0.64)
Diameter stenosis, % (SD)	14 (9)
Stent characteristics (n=235 stents)	
SYNERGY stent used, % (n)	100.0 (235)
Stent length, mm (SD)	25.0 (8.7)
Stent nominal diameter, mm (SD)	3.0 (0.5)

[a] Renal insufficiency was defined as an estimated glomerular filtration rate of creatinine clearance <60 ml/min/1.73 m^2. [b] Due to the incompatibility of software, out of 225 treated lesions, QCA was not assessed in one lesion (0.4%). BMI = body mass index; CABG = coronary artery bypass graft; IVUS = intravascular ultrasound; QCA = quantitative coronary angiography; LAD = left anterior descending; LCX = left circumflex; OCT = optical coherence tomography; OFDI = optical frequency domain imaging; PCI = percutaneous coronary intervention.

Supplementary Table 2. Differences in non-stented segments observed by intracoronary imaging.

	Vessels with diffuse disease	Vessels with focal disease	Mean difference (95% CI) [a]
Post-PCI Intracoronary Imaging	**(n=140)**	**(n=53)**	
Reference lumen area, mm^2 (SD)	6.95 (3.08)	8.32 (3.39)	**1.371 (0.537 to 2.231)†**
IVUS derived (n=134)	7.01 (3.17)	8.35 (3.68)	**1.355 (0.282 to 2.412)†**
OCT derived (n=59)	6.83 (2.90)	8.24 (2.55)	**1.369 (0.083 to 2.647)†**
Proximal Segment			
Analysable length, mm (SD)	11.24 (14.80)	12.03 (16.27)	0.754 (-3.214 to 5.157)
Analysable proximal segment	n=81	n=27	
MLA, mm^2 (SD)	5.86 (3.51)	6.59 (2.80)	0.751 (-0.322 to 1.851)
IVUS derived (n=66)	5.86 (3.65)	6.28 (2.34)	0.463 (-0.802 to 1.685)
OCT derived (n=42)	5.85 (3.35)	7.12 (3.52)	1.273 (-0.700 to 3.234)
Average plaque burden, %	49.4 (10.4)	46.3 (8.3)	**-3.120 (-6.298 to -0.051)†**
Distal Segment			
Analysable length, mm (SD)	9.30 (6.43)	8.51 (6.37)	-0.811 (-2.473 to 0.906)
Analysable proximal segment	n=102	n=39	
MLA, mm^2 (SD)	4.00 (2.65)	4.64 (2.48)	0.650 (-0.071 to 1.486)
IVUS derived (n=93)	3.91 (2.63)	4.95 (2.75)	**1.046 (0.098 to 2.054)†**
OCT derived (n=48)	4.15 (2.71)	3.76 (1.16)	-0.396 (-1.296 to 0.465)
Average plaque burden, %	41.5 (11.8)	38.0 (11.4)	-3.433 (-6.840 to 0.109)

Diffuse disease and focal disease were defined according to a μQFR-PPG index <0.78 or ≥0.78, respectively. Continuous variables are presented as mean and standard deviation (SD). [a] Confidence intervals (CI) for differences in the mean value were estimated by bootstrapping using 2000 replications. **The cross (†) after 95% CI shows a significant difference.** IVUS = intravascular ultrasound; MLA = minimal lumen area; OCT = optical coherence tomography; PCI = percutaneous coronary intervention; PPG = pullback pressure gradient; μQFR = Murray law-based quantitative flow ratio.

Supplementary Table 3. Comparison of automated quantitative echogenicity of plaque components in the target lesion between vessels with diffuse disease and those with focal disease.

	Vessels with diffuse disease	Vessels with focal disease	p value
Target lesion observed in pre-PCI IVUS	**(n=69)**	**(n=23)**	
% Total hypo-echogenic tissue	66.0 (11.8)	69.9 (7.7)	0.146
% Total hyper-echogenic tissue	9.7 (4.9)	7.2 (3.7)	0.027
% Total upper-echogenic tissue	2.0 (1.2)	1.9 (1.1)	0.850
% Total lower-echogenic tissue	13.0 (8.9)	11.9 (5.5)	0.610
Presence of calcification, %	46.4%	60.9%	0.336

Diffuse disease and focal disease were defined according to a μQFR-PPG index <0.78 or ≥0.78, respectively. Continuous variables are presented as mean and standard deviation (SD). Abbreviations as **Supplementary Table 2.**

Supplementary Table 4. Comparison of automated quantitative echogenicity of plaque components in non-stented segments between vessels with diffuse disease and those with focal disease.

	Vessels with diffuse disease	Vessels with focal disease	p value
Non-stented segment in post-PCI IVUS			
Proximal Segment	**n=49**	**n=17**	
% Total hypo-echogenic tissue	68.8 (15.9)	71.3 (15.8)	0.572
% Total hyper-echogenic tissue	7.6 (5.8)	6.1 (3.9)	0.327
% Total upper-echogenic tissue	1.4 (0.9)	1.5 (1.1)	0.588
% Total lower-echogenic tissue	11.1 (7.9)	11.9 (8.4)	0.720
Presence of calcification, %	40.8%	41.2%	1.000
Distal Segment	**n=64**	**n=29**	
% Total hypo-echogenic tissue	80.7 (11.4)	80.6 (9.7)	0.960
% Total hyper-echogenic tissue	5.1 (4.8)	4.8 (5.2)	0.796
% Total upper-echogenic tissue	2.1 (1.4)	2.9 (3.4)	0.095
% Total lower-echogenic tissue	4.8 (7.1)	4.6 (6.1)	0.914
Presence of calcification, %	18.5%	7.7%	0.333

Diffuse disease and focal disease were defined according to a μQFR-PPG index <0.78 or ≥0.78, respectively. Continuous variables are presented as mean and standard deviation (SD). Abbreviations as **Supplementary Table 2.**

Supplementary Table 5. Comparison of MLA in non-stented segments and MSA

between vessels with a post-PCI μQFR <0.91 and those with a post-PCI μQFR ≥0.91.

	Vessels with post-PCI μQFR<0.91	Vessels with post-PCI μQFR≥0.91	p value
MLA in proximal segment, mm² (SD)	4.89 (3.10)	6.39 (3.36)	0.049
MSA, mm² (SD)	5.37 (2.02)	6.02 (2.53)	0.124
MLA in distal segment, mm² (SD)	3.30 (2.03)	4.43 (2.71)	0.033

Continuous variables are presented as mean and standard deviation (SD). MSA = minimal

stent area. Other abbreviations as **Supplementary Table 2.**
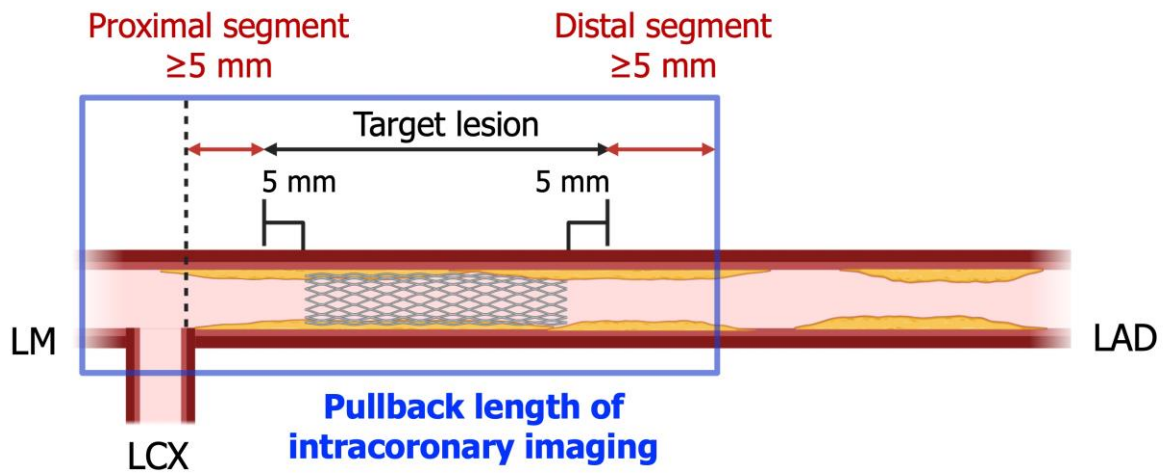
Supplementary Figure 1. Case example of intracoronary imaging analysis in non-stented segments.

Non-stented segment length had to be ≥ 5 mm in order to be included in the analysis. When the target lesion was in the left anterior descending artery or the circumflex artery, the non-stented proximal segment was analysed up to its ostium. LAD = left anterior descending artery; LCX = left circumflex artery; LM = left main coronary artery.
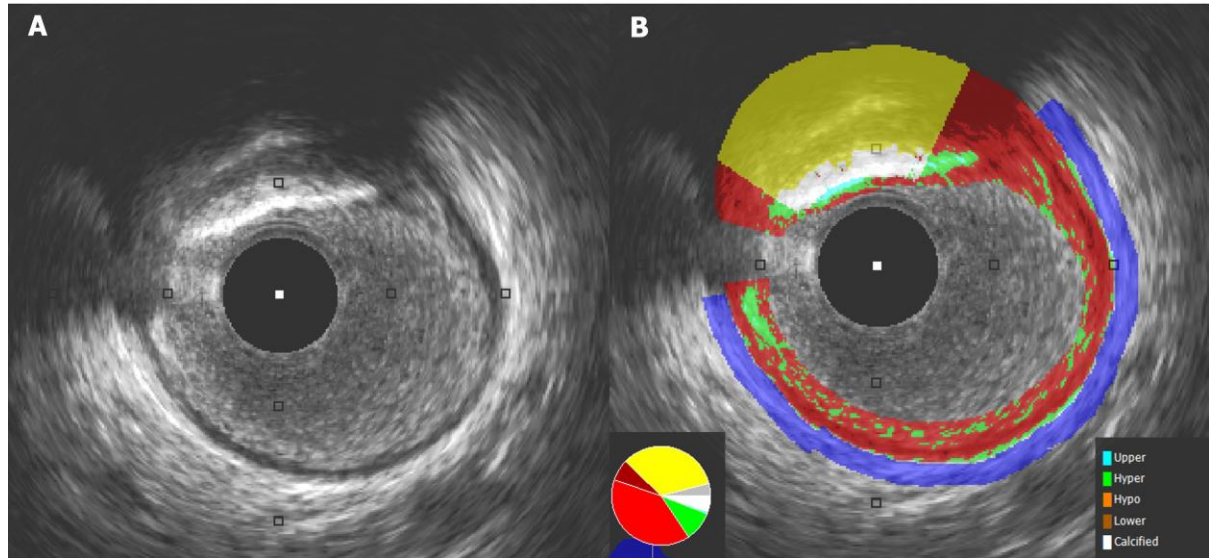
Supplementary Figure 2. Example of automated quantitative echogenicity of plaque component observed by IVUS.

According to echogenicity, tissue components — hypo- and hyper-echogenic tissue, calcification, and upper and lower tissue — were defined using the reference grey-level intensity of the adventitia (purple area). The calcifications were identified through a combination of highly echogenic tissue (white area) accompanied by radial acoustic shadowing (yellow area). IVUS = intravascular ultrasound.
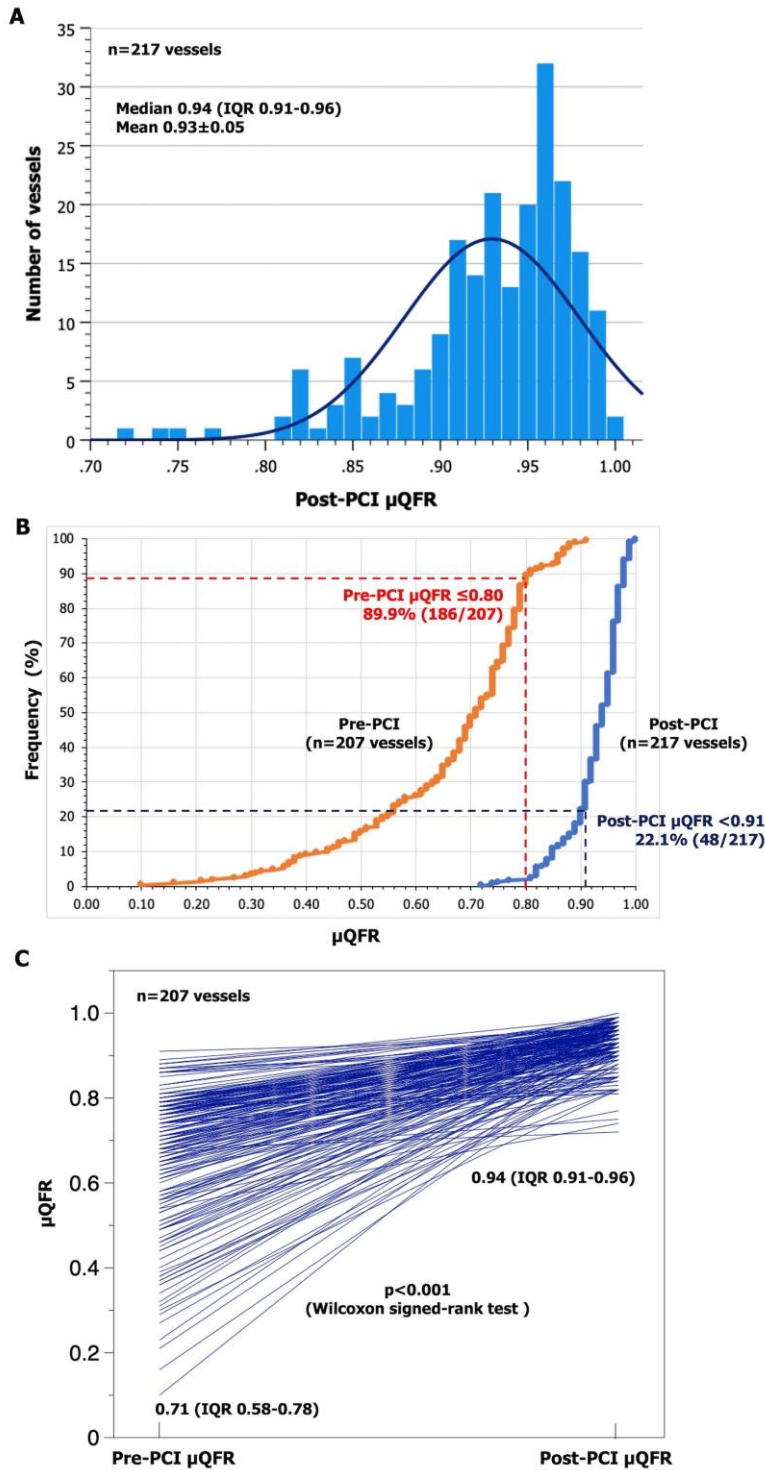
Supplementary Figure 3. Assessment of pre- and post-PCI µQFR.

Histogram showing the distribution of post-PCI µQFR (A), cumulative curves of pre- and post-PCI µQFR (B), and improvement of µQFR by PCI (C). In 207 vessels with paired pre- and post-PCI µQFR, µQFR significantly improved from 0.71 (IQR: 0.58-0.78) to 0.94 (IQR: 0.91-0.96) (p<0.001, Wilcoxon signed-rank test)(C). IQR = interquartile range; PCI = percutaneous coronary intervention; µQFR = Murray law-based quantitative flow ratio.
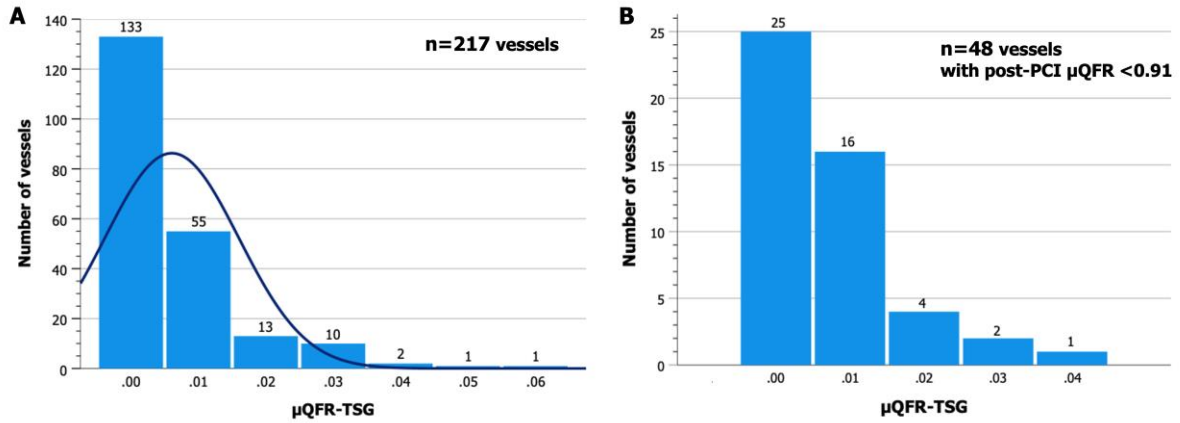
Supplementary Figure 4. Histogram showing the distribution of post-PCI μQFR-TSG.

Panel A shows the distribution of post-PCI μQFR-based trans-stent gradient (TSG) in all 217 vessels, and the median value of μQFR-TSG was 0.00 (IQR: 0.00-0.01). Panel B shows the distribution of μQFR-TSG in 48 vessels with post-PCI μQFR <0.91. Abbreviations as **Supplementary Figure 3**.